Course: Optics, Forces and Development
Santiago, Chile, January 14th - 30th, 2013

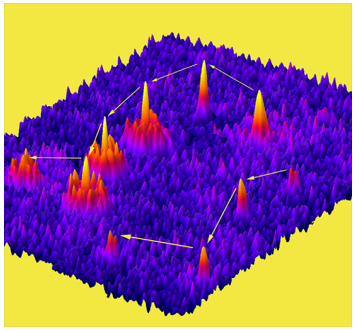

Analysis of Molecular Mobility by Microscopy

Ulrich Kubitscheck

Institute of Physical and Theoretical Chemistry
Rheinische Friedrich-Wilhelms-Universität Bonn

Fluorescence dyes light up very specific structures

Actin Cytoskeleton

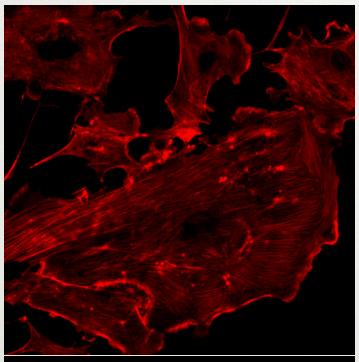

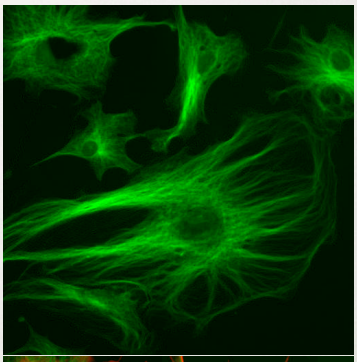

Microtubuli

Cell nuclei

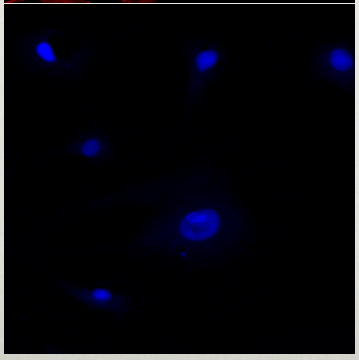

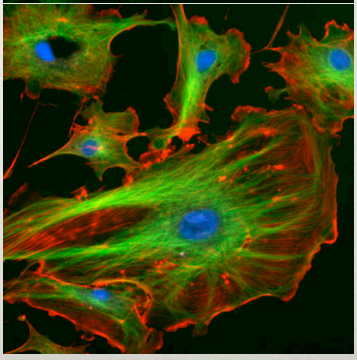

Superposition

Advantages of Fluorescence Microscopy

- specific labeling

- in vivo observation

- observation of dynamics

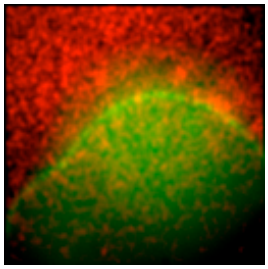

12.2 µm

green: nuclear envelope
red: transcription factors STAT1

Why should we care in the biosciences about molecular mobility?

- we can determine molecule and particle sizes: proteins, RNPs

- knowing the size, we can determine the effective viscosity

- we can see, whether active motion exists

- we can analyze transport processes in and across membranes

- we can see, whether molecules are spatially confined

- we can measure interactions: duration of binding events

Contents of this lecture

- motivation

- an introduction to Brownian motion and molecular mobility

- mobility measurements by photobleaching (FRAP)

- mobility measurements by single molecule imaging

- application example: mRNA mobility in the cell nucleus

Observation of molecular mobility

Each molecule in aequeous solution is hit 10^{13} to 10^{15} times per second by the solvent molecules: stochastic motion
This motion - the Brownian motion – is consequence of the thermal motion of the solvent molecules.

Demo of Brownian motion (here, in a gas):
http://www.falstad.com/gas/

For spherical particles in space the „Stokes-Einstein-equation“ allows to the diffusion constant:

$$D = \frac{kT}{6\pi\eta R}$$

k, Boltzmann constant
T, absolute temperature
η, viscosity of solution
R, diameter of particle

Particle transport by diffusion

Mathematica program

$$c(x,t) = \frac{1}{2\sqrt{\pi D t}} e^{-\frac{x^2}{4Dt}}$$

Start position: x=50

Distribution after 1 second:

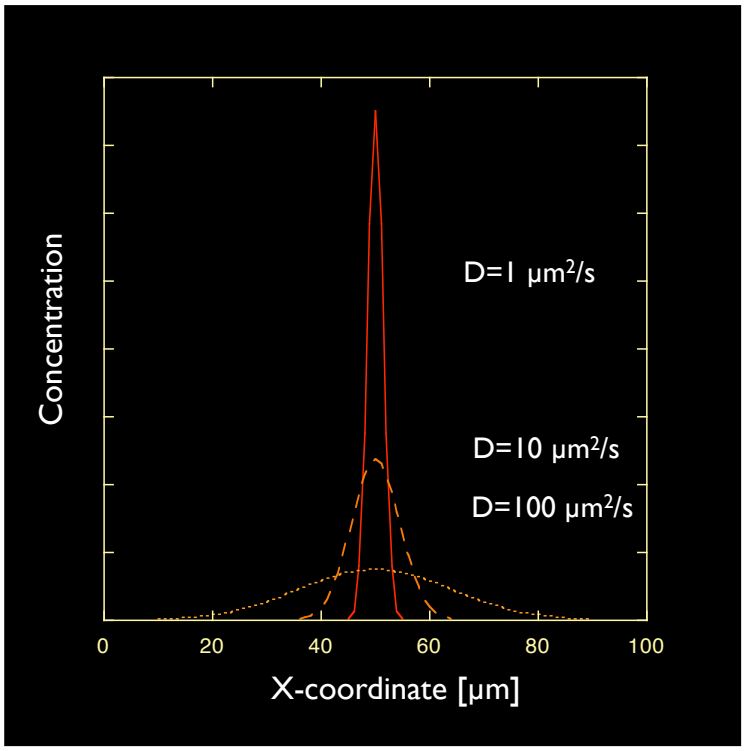

Meaning of the diffusion constant: example of membrane diffusion

Lippincott-Schwartz et al., 2001

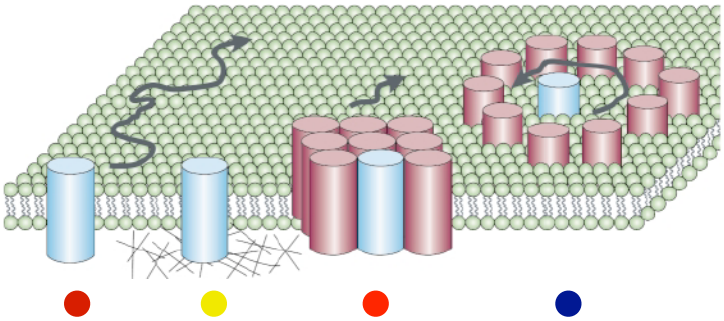

- Increase in D:
  Enhanced movement by e.g. flow
  Decrease in viscosity

- Decrease in D:
- Transient interaction with large or fixed molecules
  Formation of large aggregates (eight-fold volume → two-fold decrease!)

- Time-dependent D:
  Confined diffusion

Transport measurements by photobleaching:
Classical „Fluorescence Recovery After Photobleaching“
Abbreviation FRAP or FPR

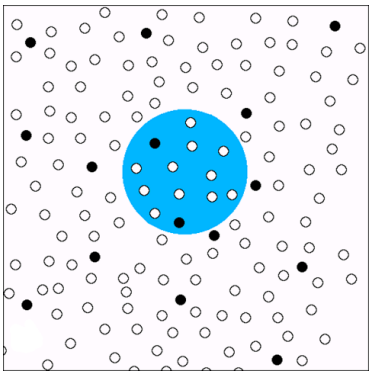

(1) Low intensity: prebleach measurement
(2) High intensity: bleaching (microphotolysis)
(3) Low intensity: monitoring measurement

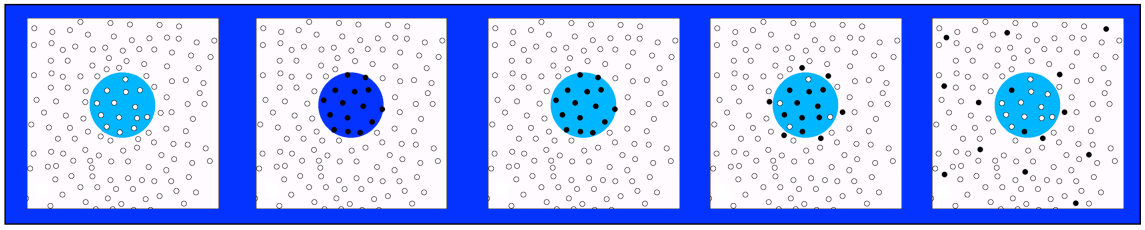

Time dependence of fluorescence in a FRAP experiment

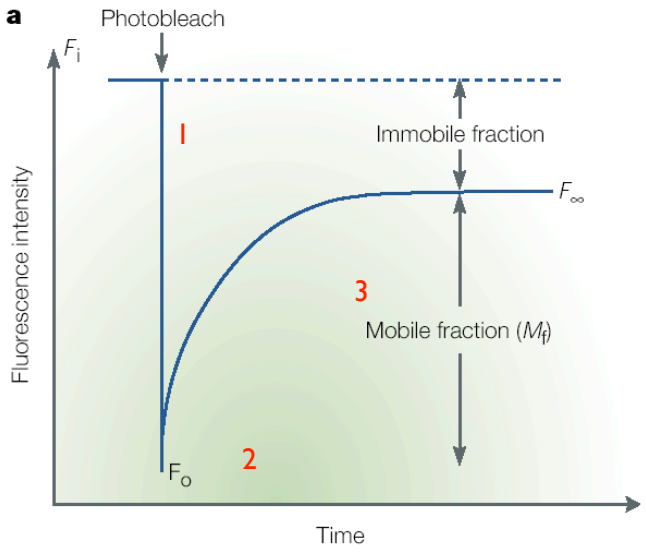

(1) Low intensity: prebleach measurement

(2) High intensity: bleaching (microphotolysis)

(3) Low intensity: monitoring measurement

Preconditions:
Instantaneous bleaching
No bleaching during monitoring

Lippincott-Schwartz et al., 2001

Mobile fraction, M_f

Determination of the mobile fraction:

$$M_f = \frac{F_\infty - F_0}{F_i - F_0}$$

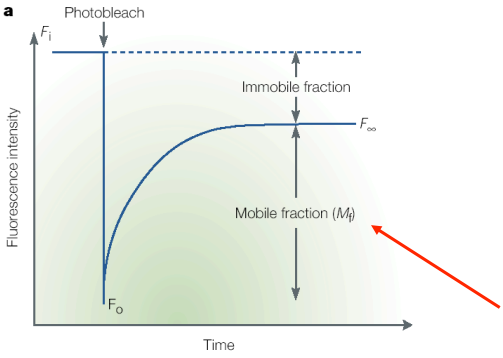

M_f=100
Molecule is completely mobile

Decrease in M_f:
Molecule binds to fixed structures or forms large aggregates
Molecule is confined to a closed compartment

Increase in M_f:
Molecule is released from restricted compartment
Molecule is released from fixed complex

Diffusion time, τ_D

Diffusion time:

$$\tau_D = \frac{w^2}{4D}$$

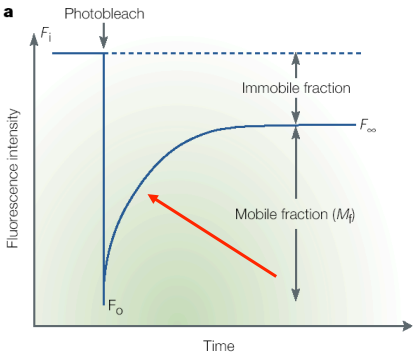

w, radius of the focussed laser beam
D, diffusion constant

τ_D is obtained plotting the recovery of the relative fluorescence intensity within a bleached area as a function of time, and by fitting this curve by a specific mathematical model

(w can relatively easy be measured or calculated)

→ determination of D

Photobleaching instrument

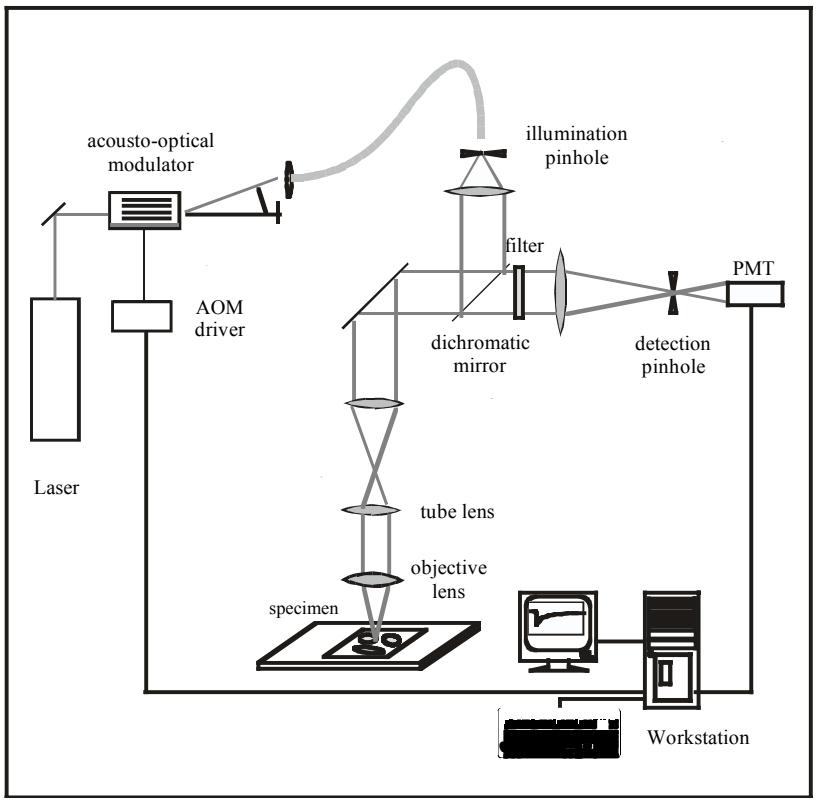

Photobleaching in a Confocal Microscope

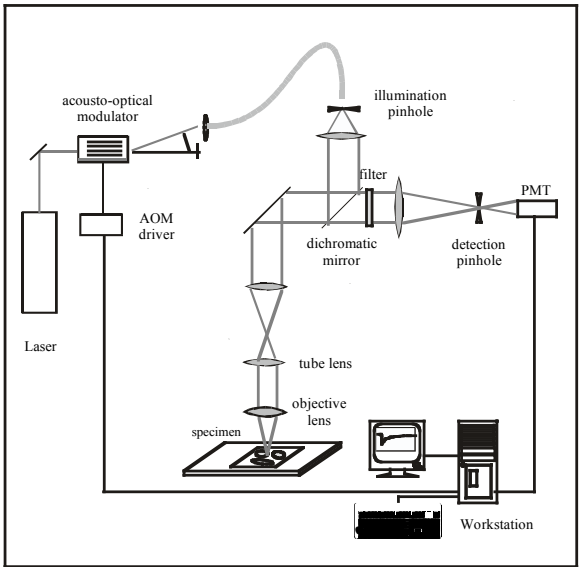

FRAP-Instrument

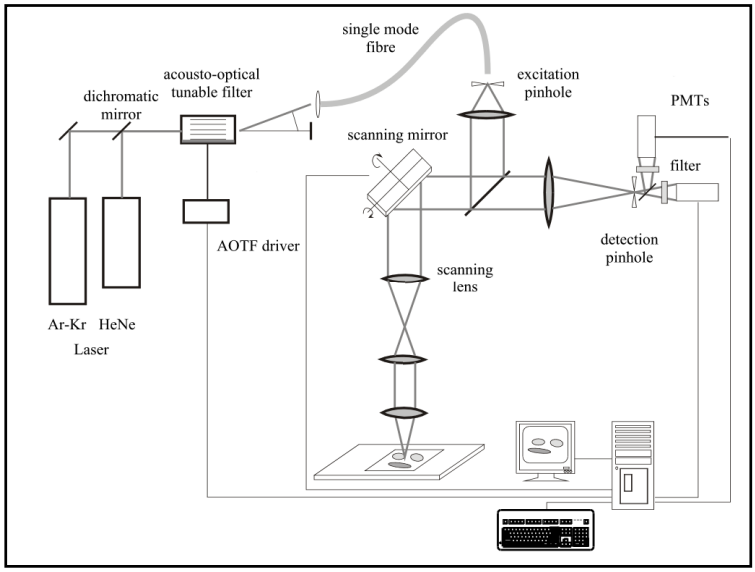

Confocal Laser Scanning Microscope

Immobile fluorescent 3D test sample

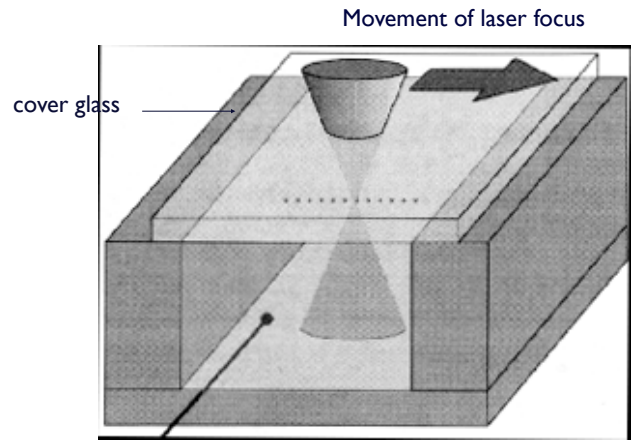

3-dimensional specimen
with fluorescein dextran (2 MDa)
in a 40% polyacrylamide gel (PAA gel)

Single-photon-photobleaching

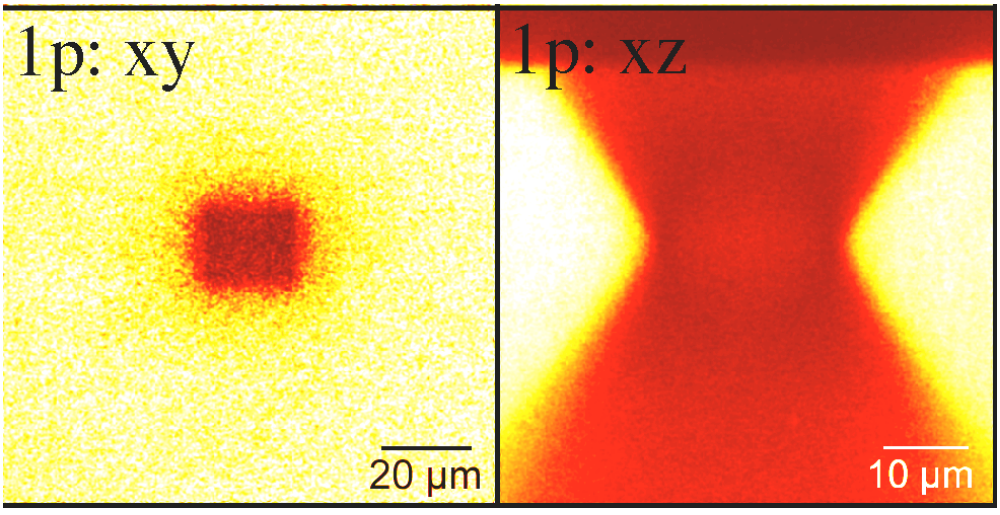

Lateral membrane transport by FRAP in the CLSM

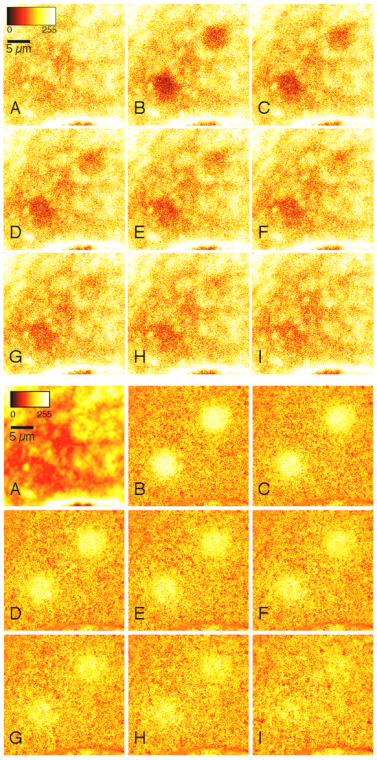

Sample:

Membranes of 3T3 cells labeled
by fluorescent lipid analoga

D = 0.2 µm²/s
Fraction of immobile molecules ≈ 5%

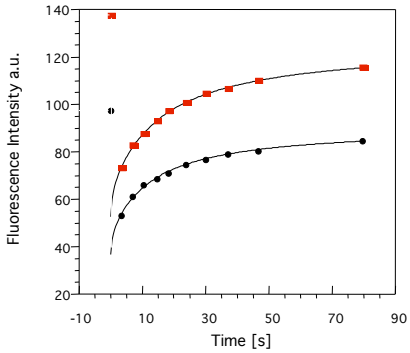

Mobility measurements by single molecule tracking

Single DiI molecules diffusing in a fluid glass-supported lipid bilayer.

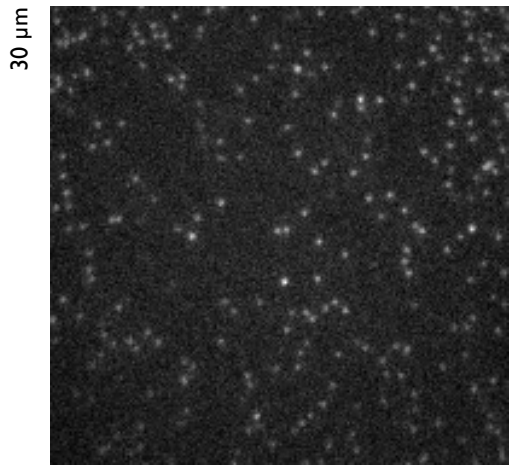

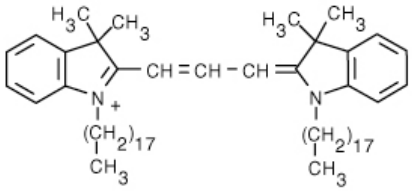

Bilayer: prepared by vesicle-fusion from dioleyl-phosphatidylcholine (DOPC) with low amounts of the lipohilic dye DiI (molar fraction of ~10^{-8}).

Image size 30 x 30 µm², recording rate 20 frames per second, display at real-time.

Movie by E. Klotzsch and G.J.Schütz, Vienna, Austria

Experimental setup

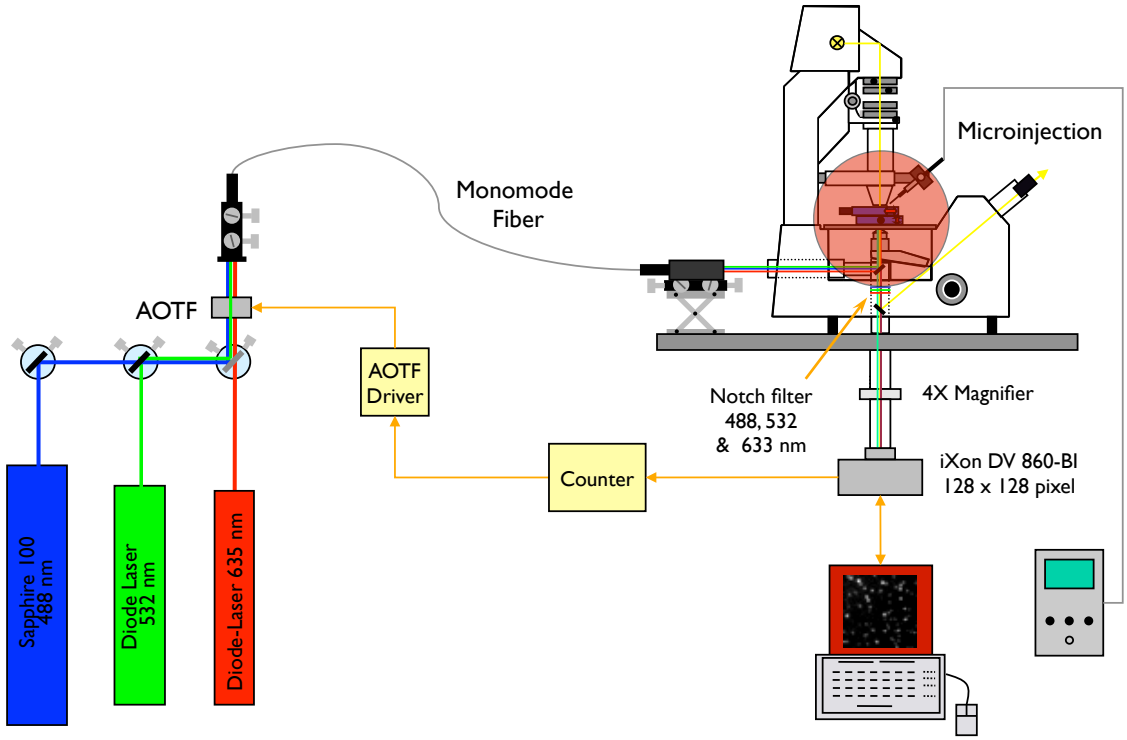

Various modes of illumination

- illuminating laser beam enters coverslip through the objective
- beam is focused on back focal plane (BFP)
- central position yields epi-illumination
- side position creates illumination by total internal reflection

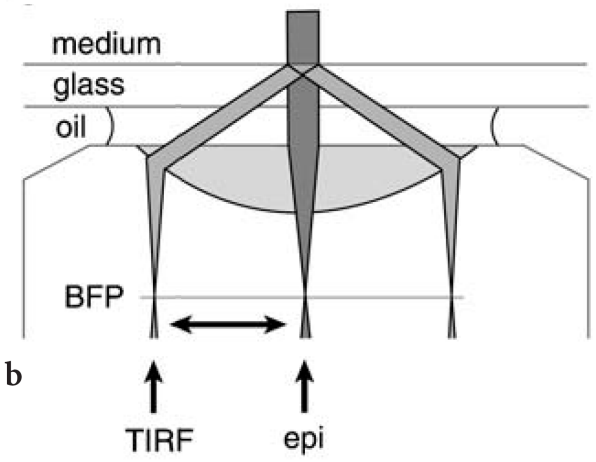

TIRF principle

=> Snellius law of refraction:

$n_1 \sin\theta = n_2 \sin\theta_T$

$\theta_C = \sin^{-1}(n_2/n_1) \quad \Leftrightarrow \theta_T = 90°$

if $\theta > \theta_C$: total internal reflection

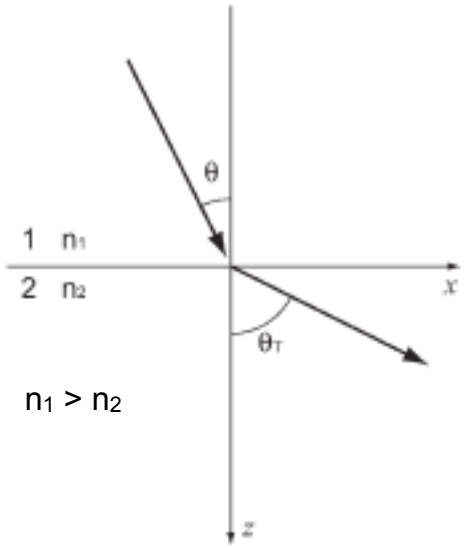

$n_1 > n_2$

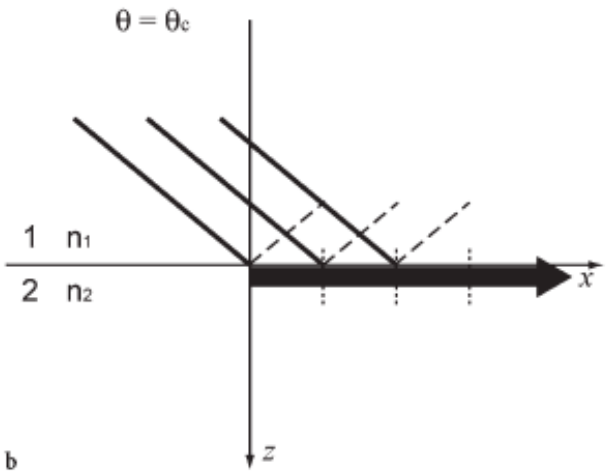

Penetration depth

Transmitted intensity $$I_T = |\mathbf{E}_T|^2 = |\mathbf{A}_T|^2 \exp\left[-z\frac{4\pi}{\lambda_2}\sqrt{\frac{\sin^2\theta}{n^2} - 1}\right]$$

Penetration depth $$d = \frac{\lambda}{4\pi\sqrt{n_1^2 \sin^2\theta - n_2^2}}$$

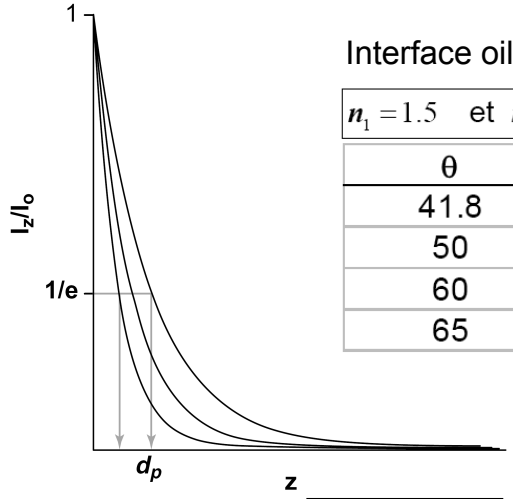

Interface oil/air

$n_1 = 1.5$ et $n_2 = 1.0 \rightarrow \theta_c = 41.8°$

θ	d
41.8	∞
50	84,4 nm
60	57,6 nm
65	51,8 nm

Interface oil/water

$n_1 = 1.5$ et $n_2 = 1.33 \rightarrow \theta_c = 62.5°$

θ	d
62.5	∞
65	170 nm
70	100 nm
75	83 nm

($\lambda = 600$ nm)

Objektiv-TIRF

- illuminating laser beam enters coverslip through the objective
- beam is focused on back focal plane (BFP)
- and shifted sidewards

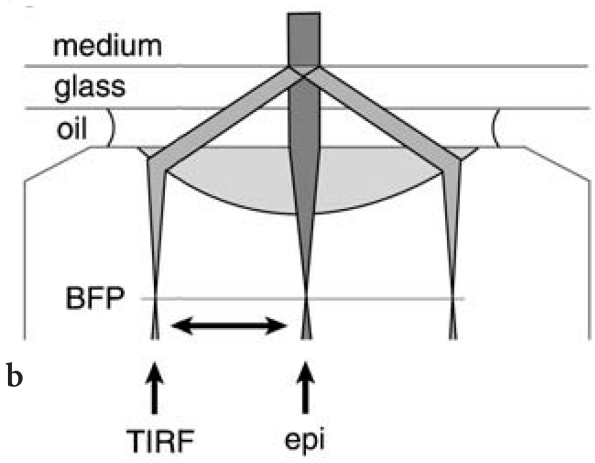

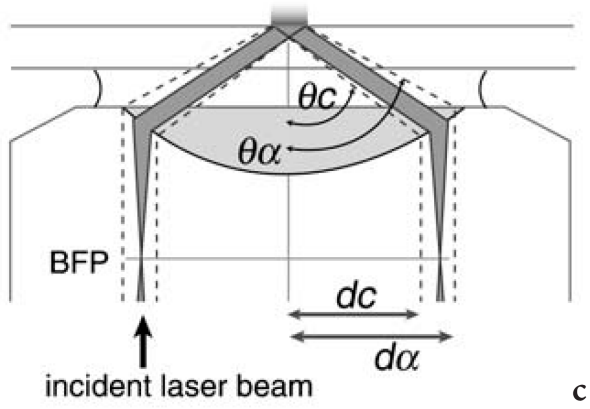

How to shift the beam sidewards

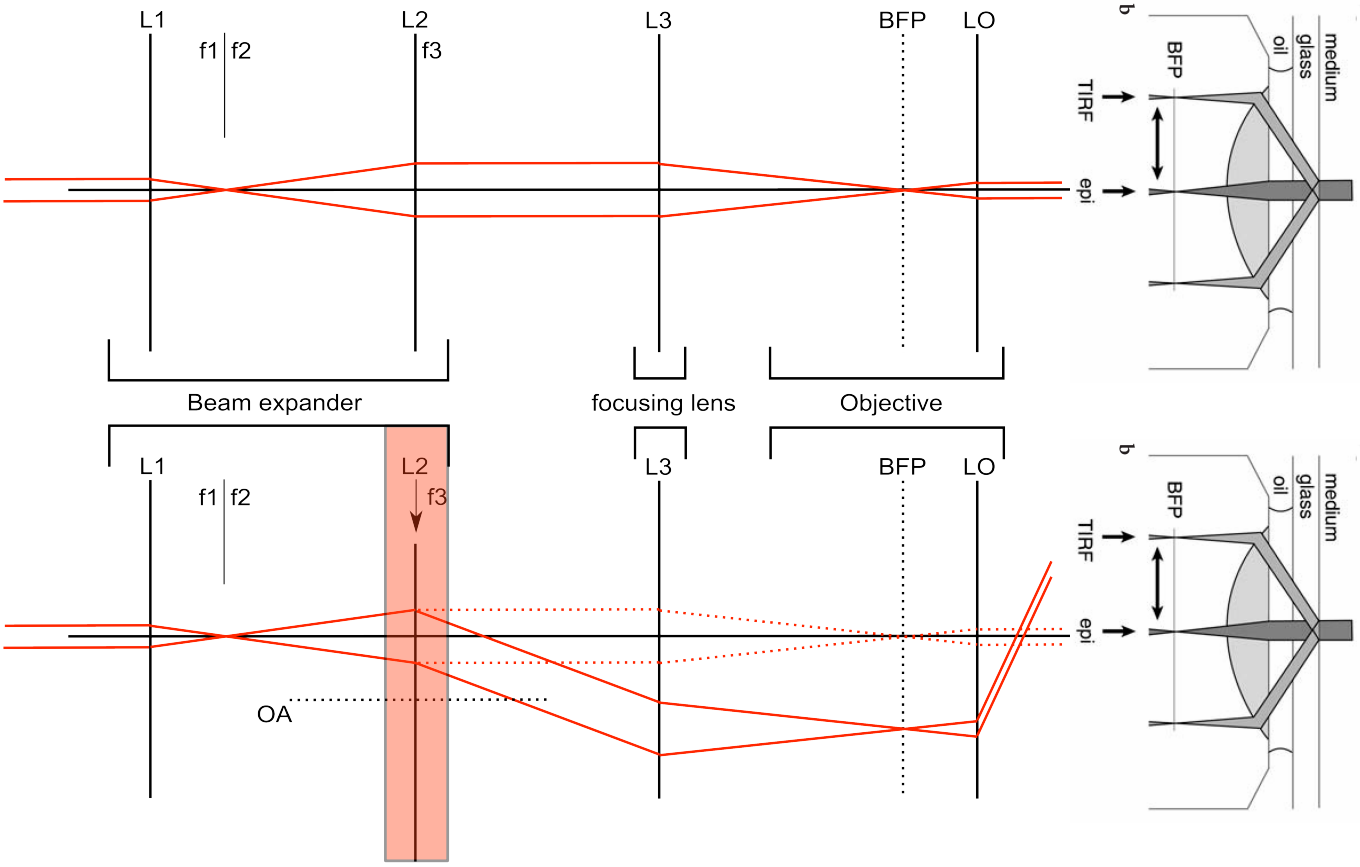

Coupling the beam via a prism

- No special objectives required; also water as immersion medium possible
- Glass hemisphere as prism allows a free choice of the entrance angle

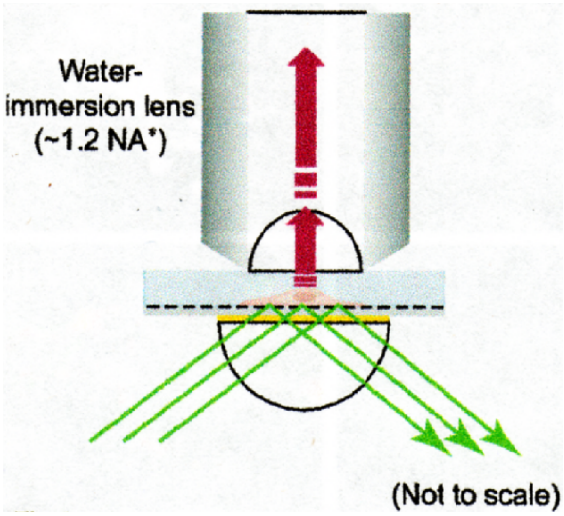

Excitation of fluorophores with TIRF

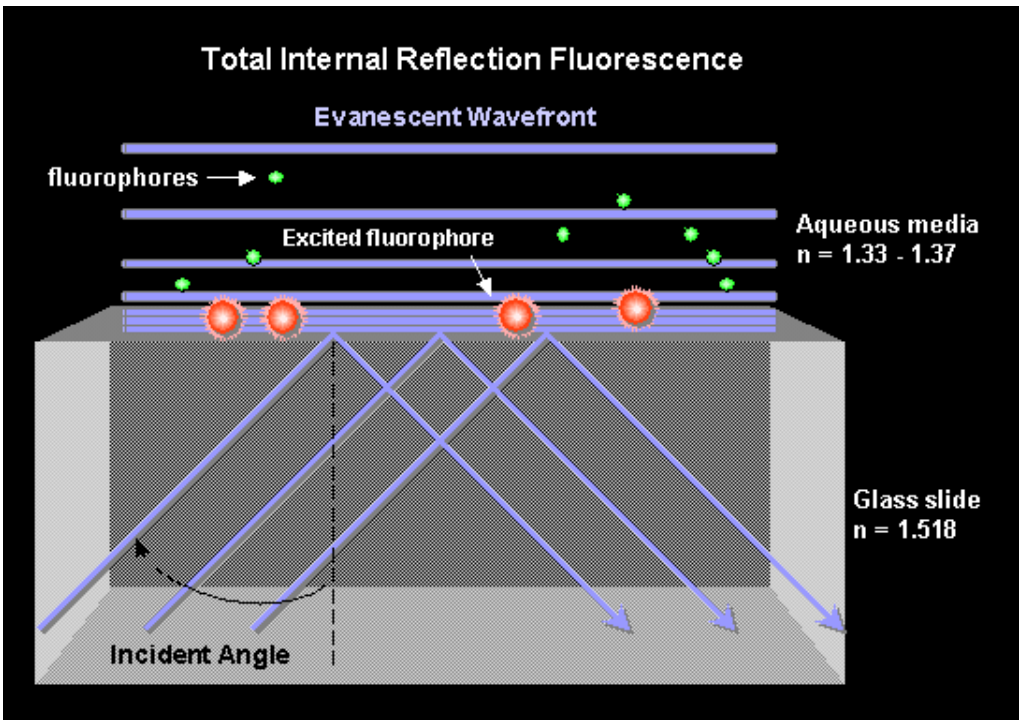

Epi- versus TIRF-Illumination

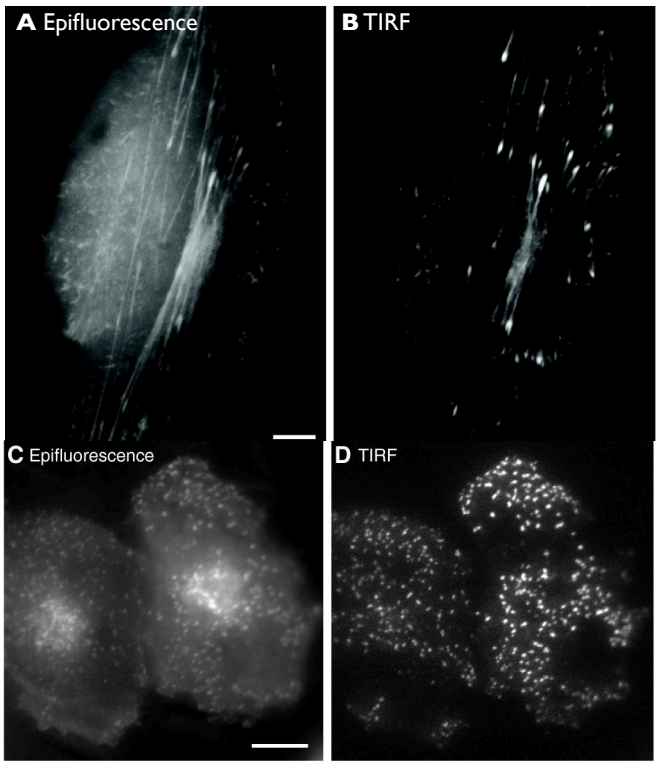

In both cases, the microscope was focused at the adherent plasma membrane. Bars, 10 μm

(**A**,**B**) Actin (LifeAct–GFP) in a migrating MDCK cell.

(**C**,**D**) Clathrin (clathrin light chain–GFP) in a HeLa cell.

Mattheyses AL, Simon SM, Rappoport JZ.
Imaging with total internal reflection fluorescence microscopy for the cell biologist
J Cell Sci. 2010 November 1;123(21):3621-3628.

Principle of HiLo microscopy

„Highly inclined and laminated optical sheet microscopy“ or „dirty TIRF“

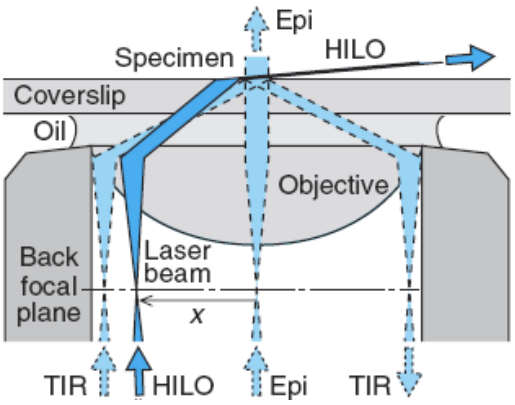

Excitation beam is diffracted at the interface of glass and sample chamber and passes inclined through the sample

Thereby, only a small section of the sample is illuminated, if the illumination field is small

Thickness of the illumination sheet

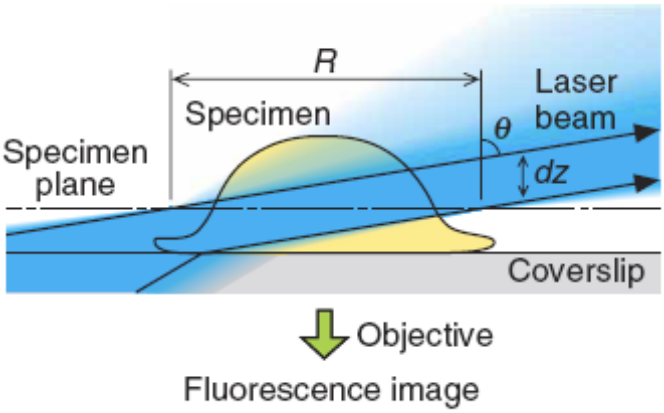

beam width dz ≈ R/tan(θ)

illumination field size, R
illumination angle, θ

Thickness of the optical dz is usually 5 to 10 µm

From EPI to HILO illumination

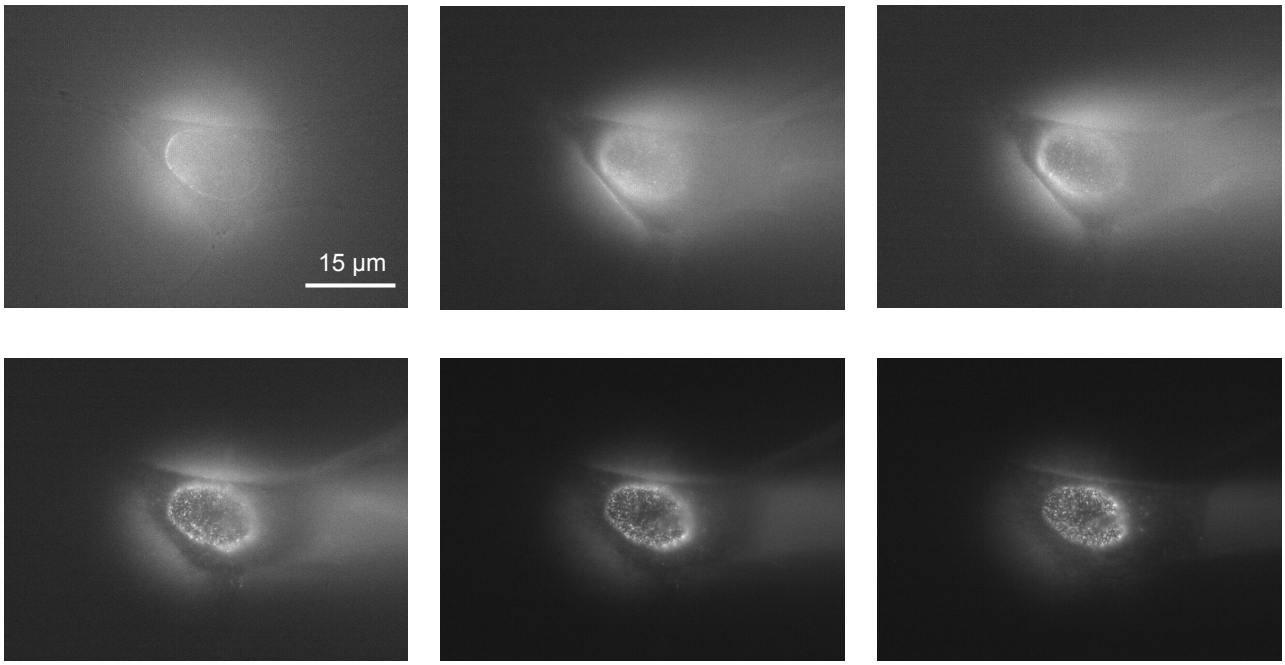

- GFP conjugated nuclear pore complexes
- Different refraction angles from EPI to HILO

Imaging of single molecules

Single, surface-attached
Oyster565 molecules
ex 633 nm, em >650 nm, 2kW/cm^{-2}, 100 ms

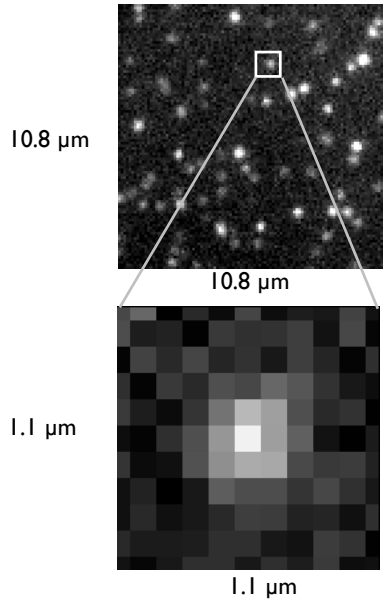

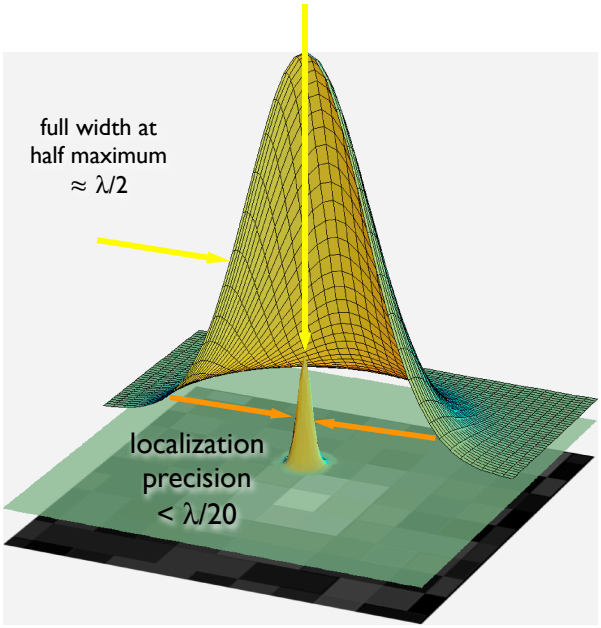

Mobility analysis in trajectories

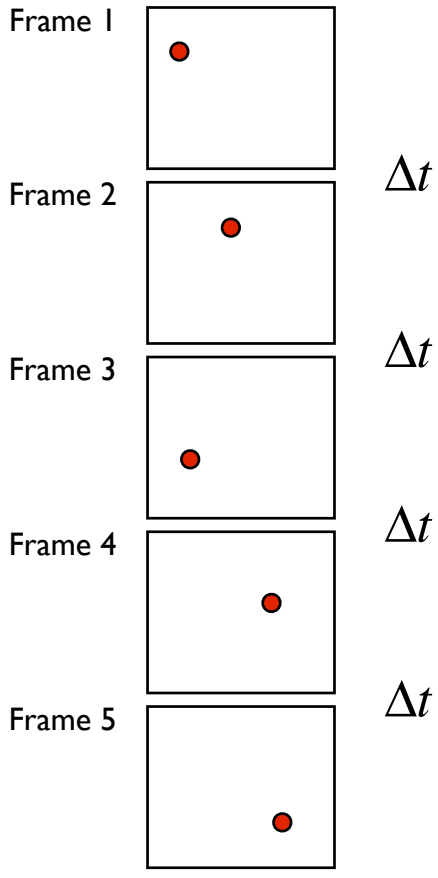

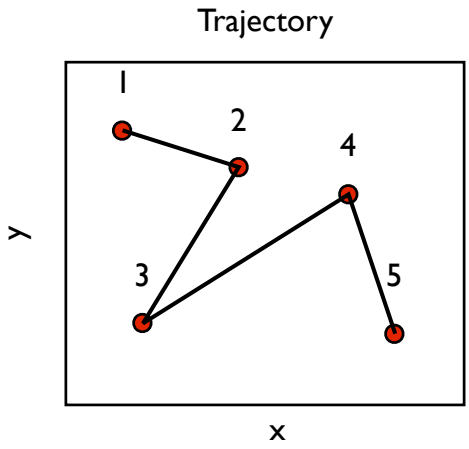

$\vec{X}(1)$ position 1

$\vec{X}(2)$ position 2

.....

$\vec{X}(N)$ position N (last one)

Mean square displacement: MSD

Trajectory

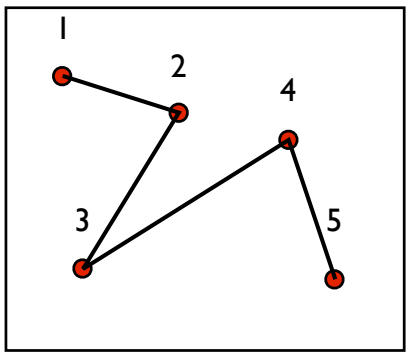

$\vec{X}(1)$ position 1

$\vec{X}(2)$ position 2

.....

$\vec{X}(N)$ position N

Displacement:

$$\vec{X}(i+1)-\vec{X}(i)$$

Square Displacement:

$$\left[\vec{X}(i+1)-\vec{X}(i)\right]^2$$

Mean Square Displacement:

$$\sum_{i=1}^{N-1}\frac{1}{N-1}\left[\vec{X}(i+1)-\vec{X}(i)\right]^2$$

$$=\left\langle \vec{X}^2 \right\rangle \quad \text{= MSD}$$

More mean square displacements

Trajectory

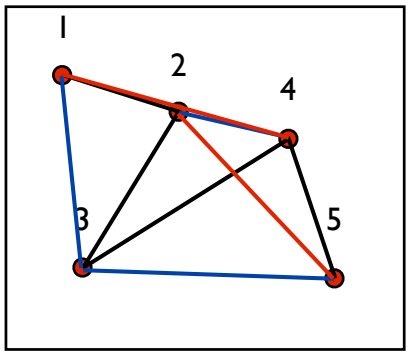

$\vec{X}(1)$ position 1

$\vec{X}(2)$ position 2

.....

$\vec{X}(N)$ position N

More Displacements:

$$\vec{X}(i+n)-\vec{X}(i)$$

Square Displacement:

$$\left[\vec{X}(i+n)-\vec{X}(i)\right]^2$$

Mean Square Displacement:

$$\sum_{i=1}^{N-n}\frac{1}{N-n}\left[\vec{X}(i+n)-\vec{X}(i)\right]^2$$

$$=\left\langle \vec{X}(n)^2 \right\rangle \quad \text{= MSD(n)}$$

$$\left\langle \vec{X}(n)^2 \right\rangle = 4D\cdot n\cdot \Delta t$$

for diffusion in a plane

Δt time lag between observations

Mobility analysis by MSDs

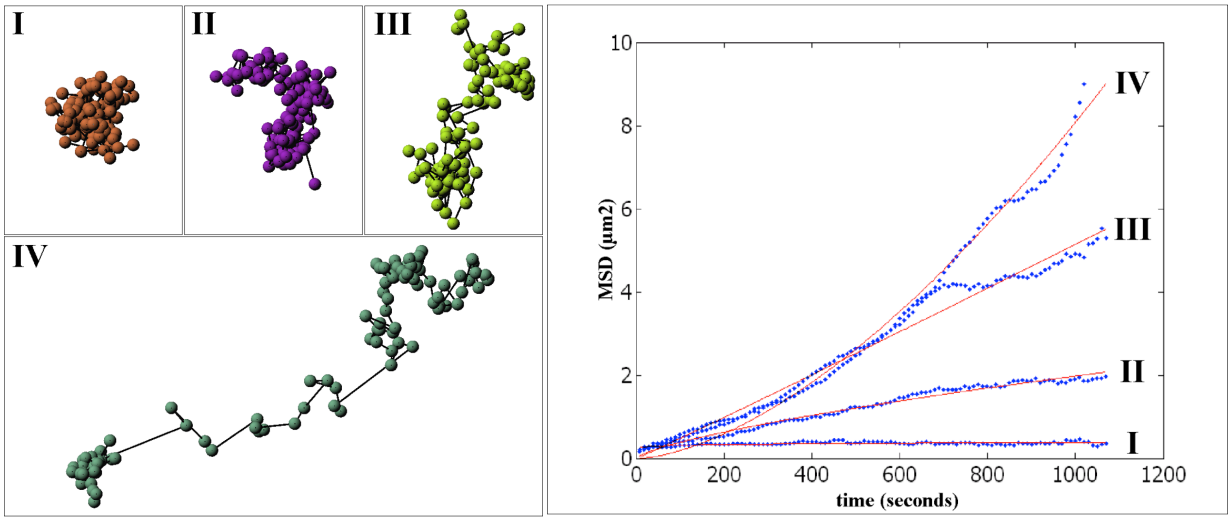

$$\left\langle \vec{X}(n)^2 \right\rangle = 2m\,D \cdot n \cdot \Delta t$$

with m = 1 for 1-dimensional diffusion
m = 2 for 2-dimensional diffusion
m = 3 for 3-dimensional diffusion

Mobility analysis by MSDs

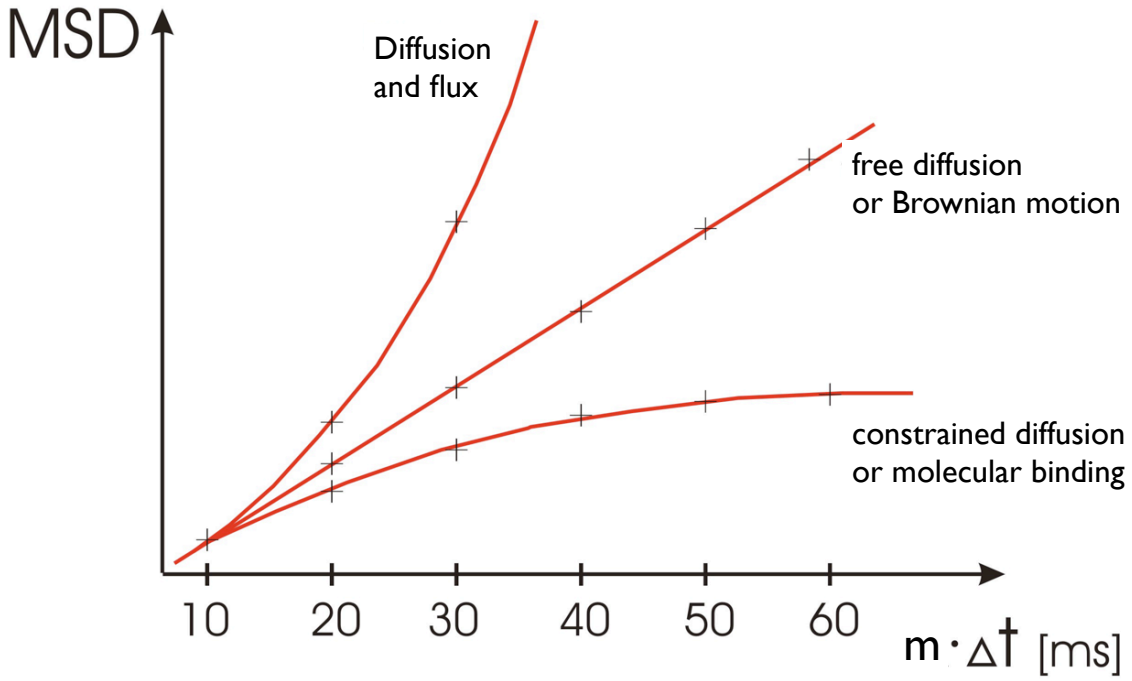

Mobile and bound particles in jump distance distributions

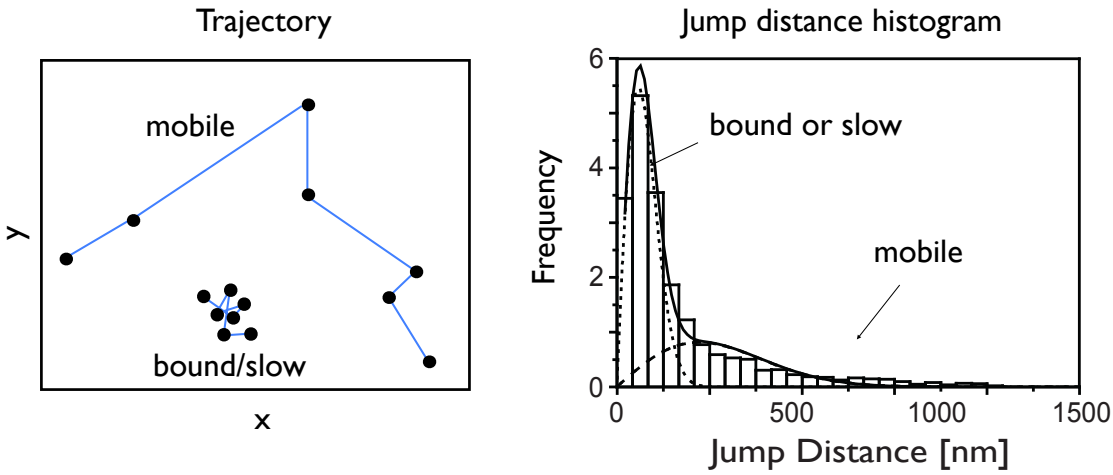

Stochastic jumps starting at the center

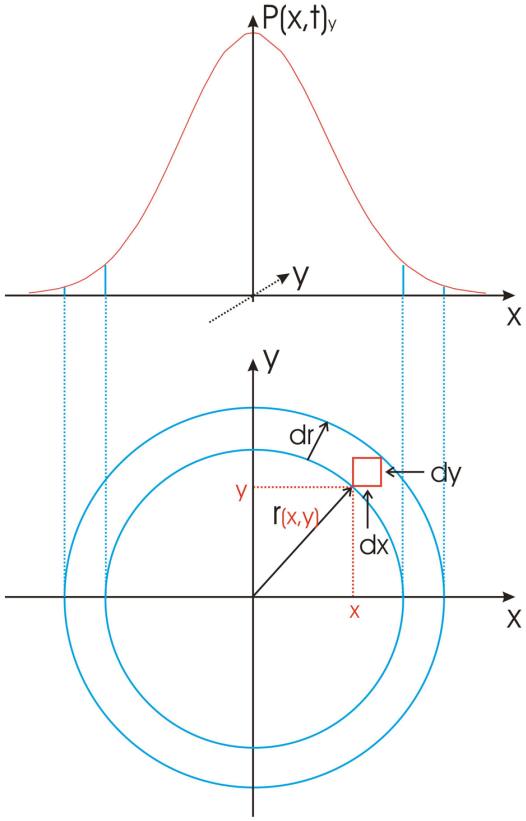

Probability density distribution function for particles jumping stochastically from 0 with diffusion constant D in time t

$$P(x,y,t) = \frac{1}{4\pi Dt} e^{-(x^2+y^2)/(4Dt)}$$

Jump **distance** distribution function:

$$P(r,\Delta t)dr = \frac{1}{4\pi D\Delta t} e^{-r^2/(4D\Delta t)} 2\pi r dr$$

Differently mobile molecules in jump distance distributions

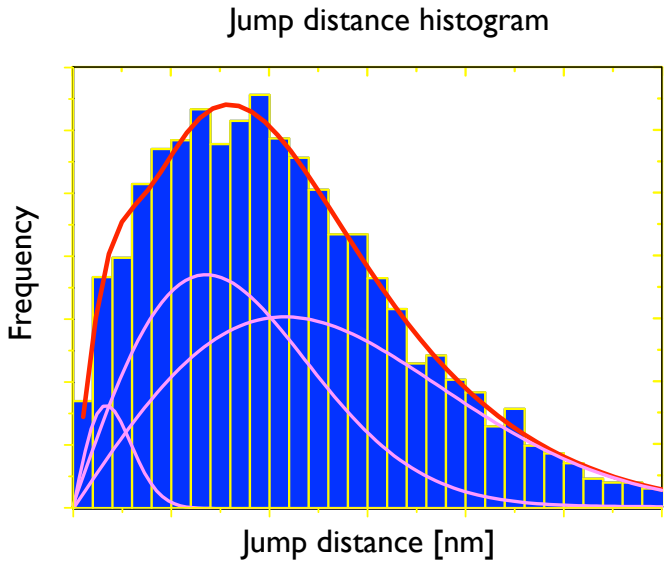

$$P(r,t)dr = \sum_{j=1}^{3} \frac{M f_j}{2D_j t} e^{-r^2/4D_j t} r dr$$

mobile and immobile fractions
diffusion coefficients
velocities
dissociation constants

Example: Single molecule analysis of RNA trafficking

specific mRNA labeling

labeling must not interfer with mRNA processing

single mRNA sensitivity

high imaging speed

high localization precision

acquisition of mRNA trajectories

understanding of mRNA trajectories

Visualization of 3D trajectories

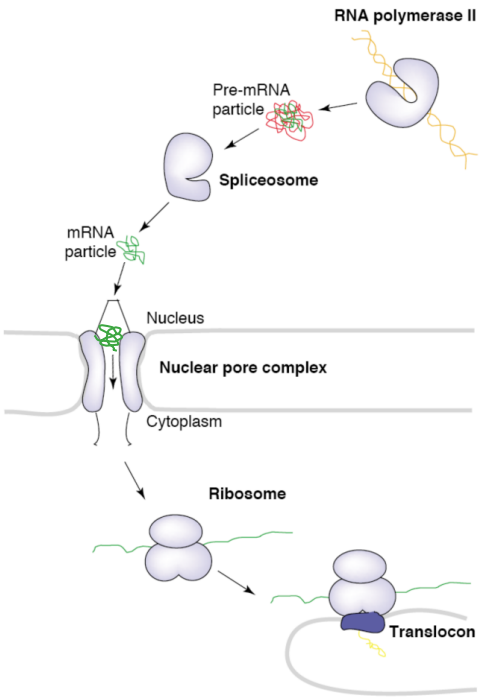

Peters (2006)

Trafficking of mRNPs in a complex intranuclear environment

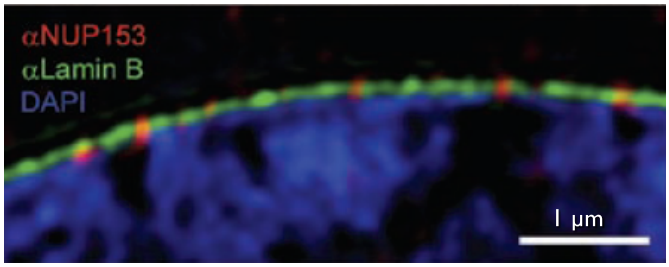

3D-SIM

Schermelleh et al. (2008)

Gene expression outcome is determined by RNA processing, trafficking and export

Contradictory results concerning mRNP mobility: D ranges from 0.03 to 7 $\mu m^2/s$

RNA-protein complexes (mRNPs) diffuse in the nucleus through „interchromatin channels“

- What happens on the „intranuclear highways“?

- mRNA export across the nuclear pore complex (NPC)

Life cycle of *Chironomus tentans*

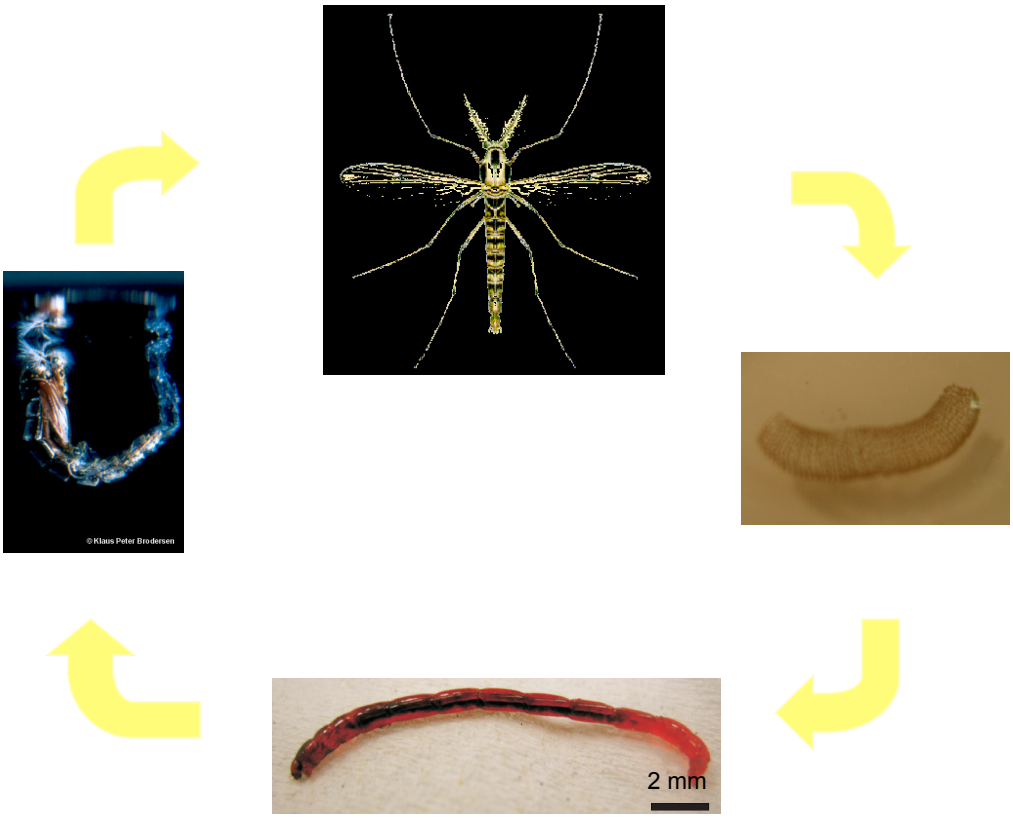

Salivary gland cell nuclei

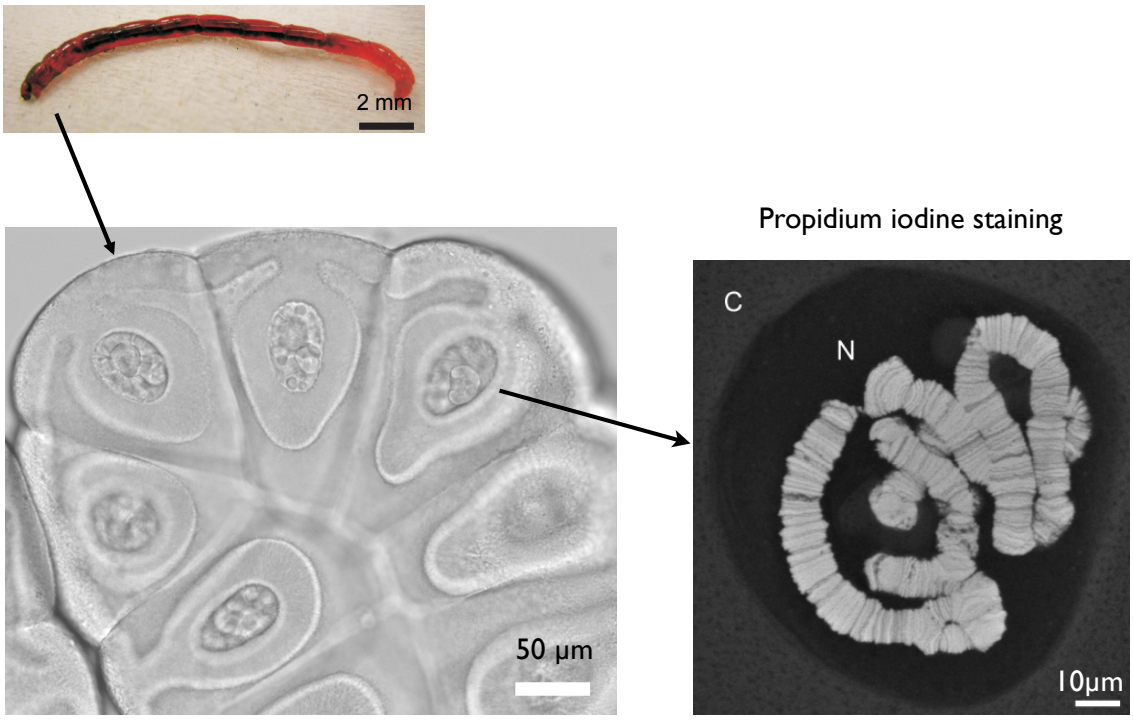

43

Balbiani Ring (BR) mRNPs

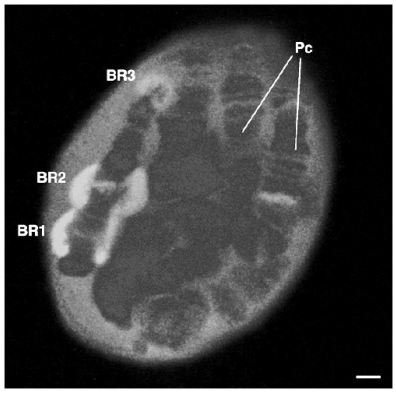

Kylberg et al. 2007

BR genes: 35-40 kb containing four short introns

Gene transcripts are packed into 50 nm mRNPs, which are translated into 1 MD silk-like proteins forming the larvae tube

Labeling by in vivo FISH or packing protein hrp36

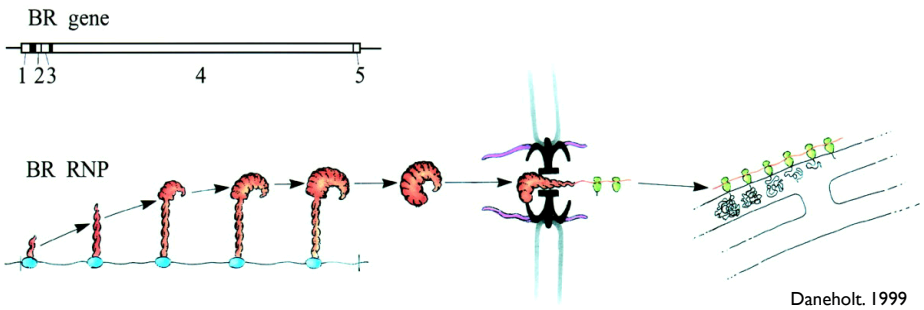

Daneholt. 1999

44

BR mRNP labeling by FISH

≈80 binding sites per mRNP for LgBR oligo

Chironomus tentans fragment from mRNA of Balbiani ring gene 2.

```
  1 ctagcaaaca cagcaaacca agcaagcaca gcaagcacag caaacctagc aagcatagca
 61 aacctagtaa acacagtaag ccagaaaaat gcggtagtgc aatgaagaga actgaagcag
121 caaaatgtgc tagaaagaat ggtagattca acagtaagag atgtacttgt acctcagttg
181 gtaaaccaag caaaccaagc aaacacagca agccaagtaa acacagcaaa ccaagcaagc
241 acagcaaacc tagcaagcac agtaaaccta gcaagcatag caaacctagt aaacacagta
301 agccagaaaa atgcggtagt gcaatgaaga gaactgaagc agcaaaatgt gctagaaaga
361 atggtagatt caacagtaag agatgtactt gtacctcagt tggtaaacca agcaaaccaa
421 gcaaacacag caagccaagt aaacacagca aacctagcaa gcacagtaaa cctagcaagc
481 atagcaaacc tagtaaacac agtaagccag aaaaatgcgg tagtgcaatg aagagaactg
541 aagcagcaaa atgtgctaga aagaatggta gattcaacag taagagaagt acttgtaact
601 cagttggtaa accaagcaaa ccaagcaaac acag
```

Sumegi, Wieslander, and Daneholt, 1982

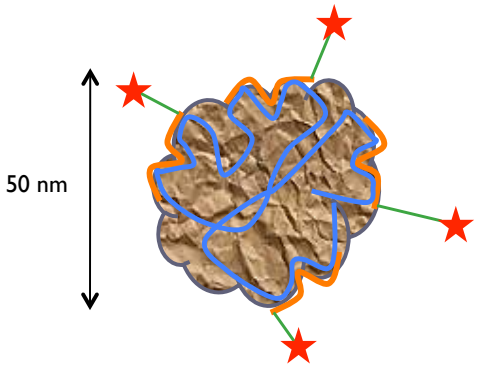

messenger RiboNucleoProtein Particle (mRNP)

mRNA

labeled oligonucleotide

packing proteins, e.g. hrp36

45

Tracking of BR mRNPs

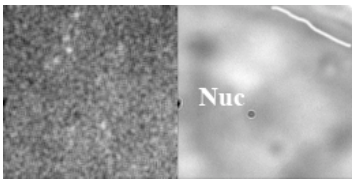

BR2 mRNPs with 50 nm diameter

Image field (12.2 µm)^2
100 Hz, display 20 Hz

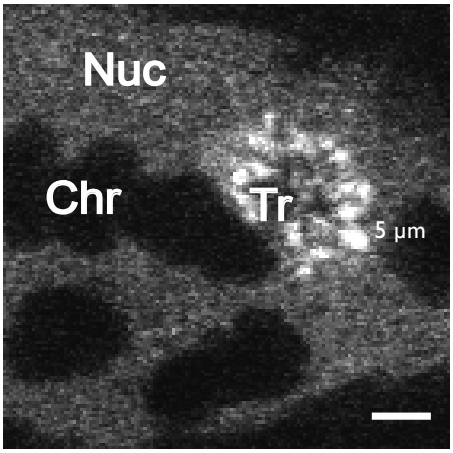

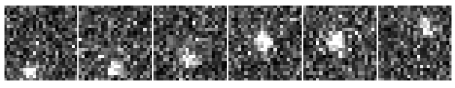

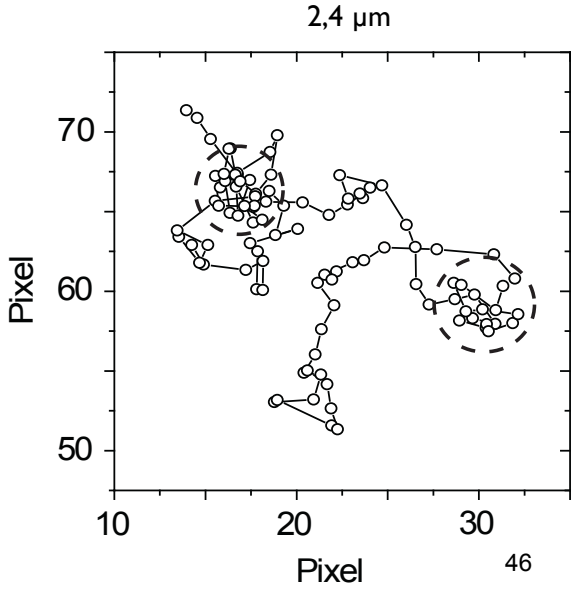

46

Jump distance analysis of single BR mRNPs for increasing time lags

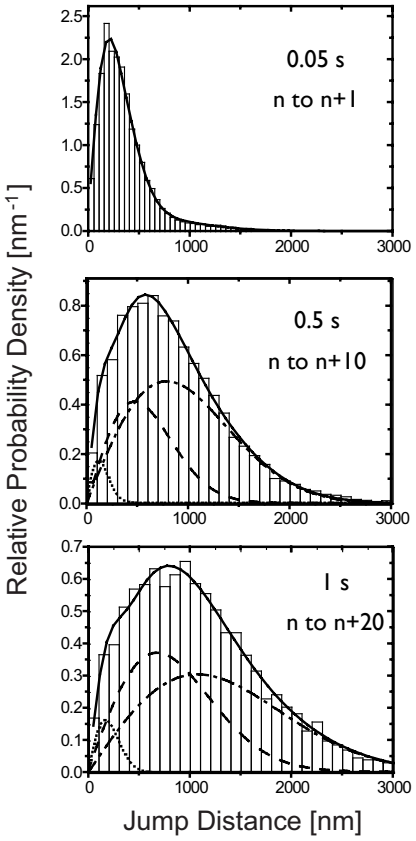

Time Lag	D_0 [μm²/s]	D_1 [μm²/s]	D_2 [μm²/s]	D_3 [μm²/s]
0.05 s	0.015 4%	0.24 25%	0.64 59%	4.0 12%
0.5 s	0.014 3%	0.22 32%	0.63 65%	-
1 s	0.015 5%	0.23 40%	0.6 55%	-

Mobility of BR mRNPs: 2 dominant mobilities

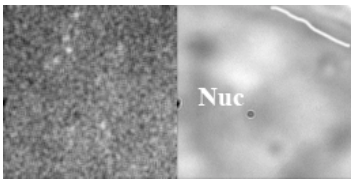

BR2 mRNPs with 50 nm diameter

Image field (12.2 μm)²
100 Hz, display 20 Hz

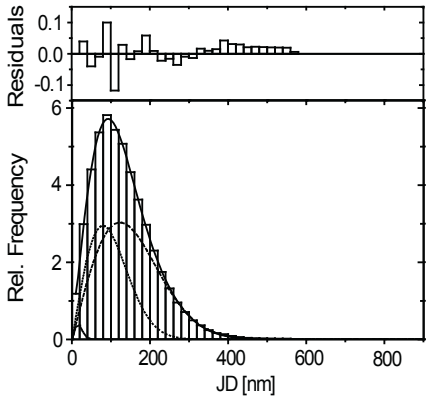

28860 trajectories
124172 jumps

40%: $D_1 = 0.3 \pm 0.02$ μm²/s
60%: $D_2 = 0.73 \pm 0.03$ μm²/s

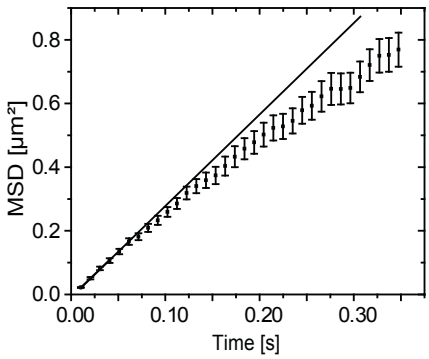

306 trajectories with >35 jumps
nonlinear MSD
$D_{in} = 0.7 \pm 0.02$ μm²/s

binding processes
or ***molecular crowding?***

500 kDa dextran molecules with 80 nm diameter

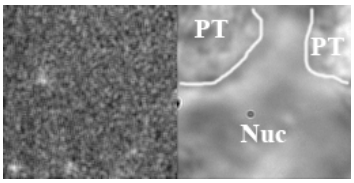

dextran-Atto647 molecules
with 80 nm diameter

Image field (12.2 μm)^2
100 Hz, display 20 Hz

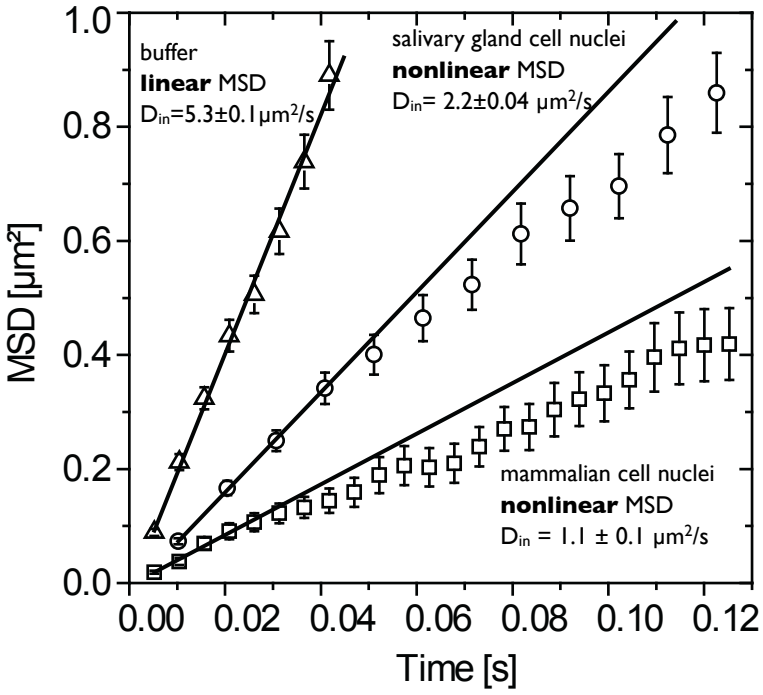

BR mRNP mobility reduced by non-chromatin structures and binding

Dextran in solution yields **linear MSD**, and **D=5.3±0.1μm²/s**

Dextran in mammalian cell nuclei yields **nonlinear MSD**, and **D=1.1 μm²/s** indicating the expected strong hindrance by chromatin

Dextran in salivary gland cell nuclei yields **nonlinear MSD**, and **D=2.2 μm²/s** indicating an unexpected hindrance by non-chromatin structures

BR mRNPs in salivary gland cell nuclei yields **nonlinear MSD**, and **D=0.7 μm²/s** indicating hindrance by non-chromatin structures ***and*** binding to these

Monte Carlo simulations indicate that diffusion combined with binding can cause a nonlinear MSD and two virtual mobility components in jump distance histograms

Acknowledgements

Biophysical chemistry group, Bonn

Lisa Büttner c
Eugen Baumgart p
Tim Kaminski b
Florian Kotzur c
Xinliang Liu b
Claudio Nietzel t
Maximilian Schiener c
Dr. Karl Schmitz c
Katharina Scherer c
Ulrike Schmitz-Ziffels c
Dr. Jan-Peter Siebrasse b
Jan-Hendrik Spille p
Andreas Veenendaal p

Former group members

Johannes Anzt c
Sarah Benter c
Claus Bier c
Dr. Corina Ciobanasu c
Sandra Cordes c
Thomas Dange b
Prof. Dr. David Grünwald bp
Enno Harms c
Dr. Andreas Hoekstra p
Constanze Husche c
Dr. Birgit Klaiberg c
Dr. Thorsten Kues p
Dr. Jörg Ritter p
Dr. Daniel Rohleder p
Dr. Jasmin Speil b
Dr. Beatrice Spottke c
Dr. Roman Veith b
Werner Wendler t

Karolinska Institutet, Stockholm, Sweden
Prof. Dr. Bertil Daneholt
Goethe University of Frankfurt, Germany
Prof. Dr. Alexander Heckel
LaVision BioTec, Bielefeld, Germany
Dr. Heinrich Spiecker, Volker Andresen

Funding by BMWi, DFG, EU and Bonn University is gratefully acknowledged